Light-Actuated Microfluidics

Unai Ortiz de Orruño Cuesta

Grupo de Transductores Químicos (GTQ), Instituto de Microelectrónica de Barcelona, IMB-CNM (CSIC), Campus UAB, Bellaterra, 08193, Spain

E-mail: unaiorru@gmail.com

Abstract. Lab-on-a-chip (LoC) technologies are nominated to revolutionize chemical and bio-chemical analysis. Although they have a great potential, they have not reached the consumer grade market, due to a lack of truly enabled functionality compared to current analytical methods. This work focuses on performing absorbance detection on LoC devices, by an easy to implement set-up. The present work is enclosed in a project which aims to combine, low-price absorption detection, low-cost materials and fast prototyping/fabrication methods for developing an affordable and portable diagnostic tool based on enzymatic immunoassays. The obtained results are satisfactory, due to the obtained sensitivity, an order of magnitude higher than a standard microplate reader.

Keywords: Microfluidics, lab-on-a-chip, optical detection, absorbance, sensor integration.

1. Introduction

Microfluidics is the manipulation of fluids at the submillimetre scale. A. Manz proposed in 1990 the use of this technology for developing 'miniaturized total analytical systems (μ-TAS)'[1] also known as Lab-On-Chip (LoC). This attempt has a clear goal: not only reducing the analytical systems size but improving the analytical performance while decreasing the sample and reagent volume. Thus, LoC devices for chemical and biochemical analysis are nominated to be revolutionized, especially clinical diagnosis,[2-6] pollution test[3-4] and quality controls[7].

Traditionally, LoC and clean-room have been closely connected, which requires specialized skills and expensive equipment.[8] For tackling this obstacle, LoC community is looking for new fabrication methods and materials.[9] Fast prototyping methods[10-12] and plastic materials[11-13] are in the spotlight for achieving low-cost LoC fabrication techniques.

Although LoC devices promise many advantages in chemical and biochemical analysis, nearly three decades after μ-TAS was introduced for the first time, LoC devices have not reached the costumer grade market. The lack of a 'killer application'[14], one that shows companies that microfluidics are not a potential market but a real ensemble of solutions, could be the reason. Other cause could be that LoC devices, by definition, are not designed for generating high revenues.[2] The introduction of truly enabled functionality

compared to current methods is the key for reaching the costumer grade market, although obtaining low-cost, sensitive and portable analyte detection microfluidic systems is difficult.

Moreover, the necessity of external fluidic handling elements such as valves and pumps is blocking the development of portable LoC based platforms. Wax microvalves are a candidate for becoming a fluidic control standard. The working principle consist on blocking a microchannel with wax plug and making it melt for opening the channel. When the wax is melted, it is displaced. Although this valves are cheap and easy to integrate, they can be actuated only once, as the valve is closed until it is actuated, which makes it to be continuously opened. Electrically[15] and optically[16] actuated wax microvalves capable of multiple actuation have been recently introduced by GTQ. In these valves the whole wax plug is not melted. The optical controlled ones are specially promising, as the only external hardware needed is a LED.

Optical detection; which includes fluorescence, chemiluminescence, absorbance and surface plasmon resonance (SPR); is thought to be one possible solution for developing a sensitive analytical microfluidic system, because of its synergy with LoC devices. Between the introduced optical detection methods, absorbance is the cheapest and the easiest to implement in a portable device solution.[17] Fluorescence, chemiluminescence and SRS present a high sensitivity, but they need large detection systems (poor portability).

The major drawback of absorbance-based detection in LoC devices is that its short optical path decreases the sensitivity, as Beer-Lambert law describes. Many attempts have been done for increasing the optical path, as integrating waveguides,[18-19] the use of mirrors[20] or solutions that contain multiple selectable paths.[21] Despite those trials, a short optical path has allowed precise absorption measurements by using optical fibres for connecting the light source and the detector.[22] In addition, Samsung commercialised its lab-on-a-disc device[23-24] using short optical path absorbance measurements.

In the present work, a low-cost absorbance-based optical detection system for LoC devices based on a LED-photodetector pair is introduced. This work is part of a project that aims to develop low-cost LoC devices for microbead-based diagnostic assays.[23, 25-26] Thanks to the high surface/volume ratio of the microbeads the sensitivity of these assays is very high allowing for absorbance measurement in short path-lengths (i.e. microchannel height). LoC devices are fabricated using a cost-effective and fast prototyping technology based on plastic films (lab-on foil). Fully integrated optically actuated wax valves[16] enable the manipulation of microbeads inside the microfluidic structures, which is key for the development of integrated bead-based bioassays.

2. Experimental

2.1. Detection system

A LED-photodetector pair was used for absorbance measurements. As illustrated in Fig. 1, the LoC is illuminated with a red LED (650-670nm). Emitted light goes through the LoC as microfluidic channels are covered by transparent layers and reaches the photodetector. Signal arriving to photodetector varies when the sample inside the LoC changes, as the absorbance changes.

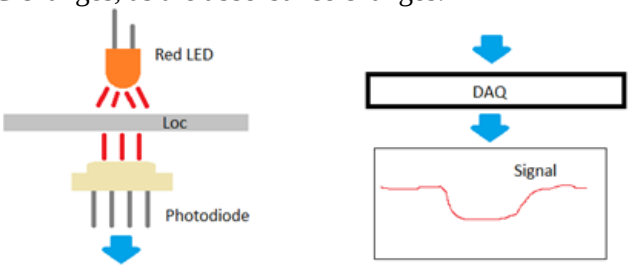

Figure 1. Schematic representation of the employed detection system. A sample go through a LoC device while it is illuminated by a red LED. Light arriving to photodiode changes according to sample absorbance. The signal is recorded by a Data Acquisition board (DAQ) which sends the data to a PC.

The detection system is designed for detecting blue coloured solutions. LED's emission spectrum was chosen to fit oxidized 3, 3′,5 ,5′-tetramethylbenzidine (TMB) absorption peak (653nm). TMB is one of the most widely used enzymatic substrate for enzymatic immunoassays. TMB gives a blue coloured product when reacted with hydrogen peroxide. The employed photodiode has a maximum responsivity in red and infrared wavelengths, for maximizing the sensibility.

Red LED emission intensity was controlled from a PC by a Digital to Analog Converter (DAC). It was connected in series to 20kΩ resistance (R_1) for controlling the current. The photodiode contains a 1MΩ resistance (R_f), that allows to covert the photodiode's current (the signal) into a voltage value, as described in *(1)*, that can be treated as a signal. This signal arrives to an Analog to Digital Converter (ADC). The ADC sends the data to a PC. The Fig. 2 shows the described circuit. A Data Acquisition board (DAQ) was acting as DAC and ADC at the same time. All the system was controlled by LabView2013.

$$V_{Signal} = -R_f \cdot I_{Photodetector} \qquad (1)$$

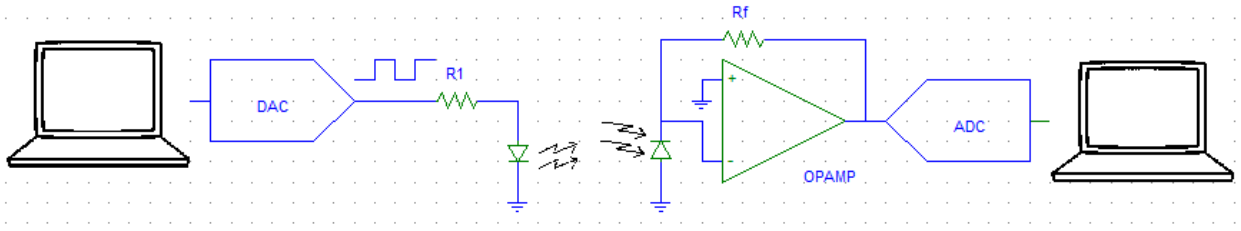

Figure 2. Schematic representation of the data acquisition circuit. A PC by a DAC controls the light emitted intensity of the LED. R_1 controls the current arriving to photodiode. Photodiode is connected to a trans-impedance amplifier, composed by OPAMP and R_f. Obtained signal is send to a PC by a ADC.

2.2. Chip fabrication

The microfluidic chips used in this work comprise one structured double-sided adhesive layer (PSA) sandwiched between two polyester transparency films. The bottom polyester film incorporates the printed black ink lines required for valve actuation. The top transparency film includes the holes for fluid access.

The design of the microfluidic chip was performed with CorelDRAW X7. A cutter plotter cuts the design on PSA, creating the microchannels. The cut pattern must be removed using a scalpel. Next, the transparencies are stuck to the PSA. The bottom film must have the black ink lines pointing the cut pattern.

Wax valves were easily fabricated at the desired locations within the microchannels by the deposition of solid beewax on the substrate before the chip assembly. Once both films are stuck sandwiching the wax, chip must be heat up, melting the wax, for achieving the final valve. Finally, liquid reservoirs were added using cut pipettes and silicone.

2.3. Wax Microvalves Working Principle

Wax valves were designed for opening when a pressure difference greater than 3 kPa is applied across the barrier and for closing at zero pressure[16]. A wax plug is placed on the microchannels, Fig. 3 (*a*). A black ink line (photothermal heater) is printed on the plastic substrate, for microvalve actuation. The black ink line printed on the substrate is positioned perpendicular to the wax barrier extending on both sides of the wax structure. The temperature of the photothermal heater raises when illuminated with a LED. The wax is in direct contact with the heater, which makes the wax to heat up and melt. Only the wax in direct contact will melt. If a pressure difference is applied between the two valve's faces, the melt wax will displace, creating a channel across the wax barrier as illustrated in Fig. 3 (b) and (c). The opening of the valves can be modulated by applying a short light pulse (small-tunnel partial opening) or a long light pulse (full-microchannel opening), Fig. 3 (b) and (c) shows them respectively. This unique property enables the manipulation of microbeads inside the microfluidic structures, which is key for the development of integrated bead-based bioassays.

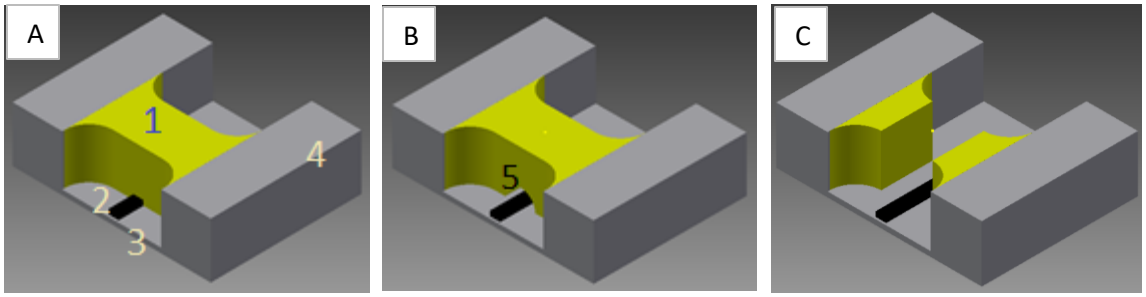

Figure 3. Schematic representation of employed wax microvalves. a) Closed wax microvalve. b) Partially opened wax microvalve. c) Completely opened wax microvalve. Yellow bulk (1) represents beeswax and black-line (2) the optical heater. 3 and 4 illustrate the bottom polyester transparency films and the PSA, respectively. Top film does not appear on the scheme. 5 indicates the small-tunnel due to partial opening.

For closing the microvalve, optical heater must be heated up, but no pressure difference must be applied. In this case, wax will be melted as well, but it will cover the previously created channel. Only partially opened microvalves can be closed.

3-100kPa is the pressure range in which microvalves open and close properly. Opening partially a microvalve has an energy consumption of 0.3J; closing needs an energy of 0.6J and 1J in air and water, respectively. Opening completely needs 4.5J. White LEDs where used for controlling the valves, as a black optical heater was used.

2.4. Chip design

A simple microfluidic chip comprising 3 reservoirs, 3 microvalves and an outlet/detection channel was designed to test the detection system, Fig.4 (a). In analytical LoC devices, dead volumes can cause distortions on the detection, as it can cause sample mixing with mentioned volumes. For minimizing dead volumes, valves are placed as close as possible to the central channel. On the chip, reservoir *6* must always contain the blank, as after any measurement the long channel must be cleaned with blank.

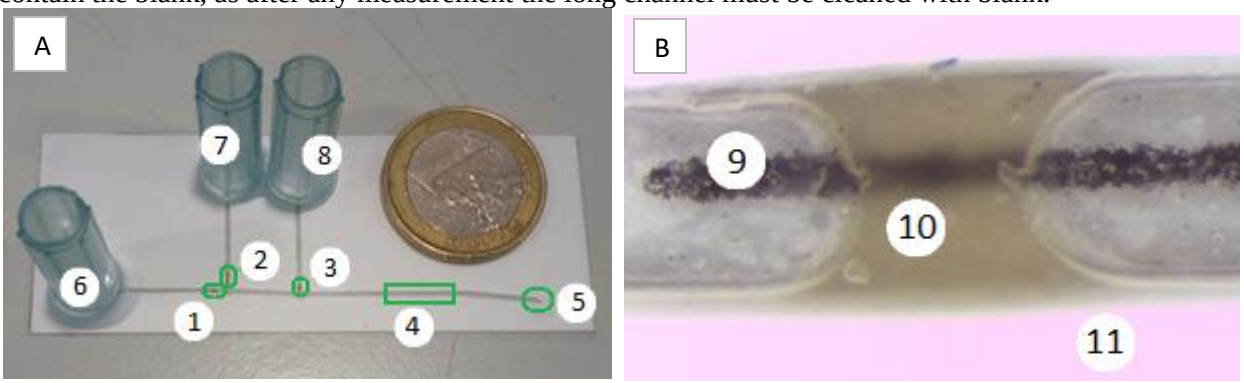

Figure 4. (a) An assembled chip. 1, 2 and 3 indicate the valves. 4 is the detection area. 5 shows the outlet hole. 6, 7 and 8 indicate the liquid reservoirs. (b) An assembled wax-valve. 9 indicates the printed black ink line (optical heater), 10 the valve's wax and 11 the PSA.

The LoC chip is designed for being a platform for bead-based enzymatic immunoassays, using horseradish peroxidase (HRP) as label and TMB as enzymatic substrate.

In order to facilitate the optimization of the detection system (avoidance of the enzymatic reaction) in the present work, a blue dye with similar absorbance spectrum of TMB oxidation product was used. For performing these measurements, negative pressure is applied in *5*, Fig. 4 (a), by the use of a micropumping system. There will not be flow till one valve is opened. On that moment, the liquid contained in the reservoir connected to that valve will pass through *4*, Fig. 4 (a), where the measurement will be done, and will leave the chip at *5*, Fig. 4 (a). For closing the valve, no pressure must be applied in *5*, Fig. 4 (a). After any sample

measurement, blank must pass through *4*, Fig. 4 (a), for cleaning. To get an optimum cleaning, blank must be placed in reservoir *6*, Fig. 4 (a). For allowing valves to close, they must be partially opened.

Enzymatic immunoassays aim to detect an antigen. For performing them, HRP is conjugated with a detection antigen and the beads coated with capture antigen. Coated microbead solutions are injected in reservoir *7* (blank) and *8* (sample), Fig. 4 (a). By partially opening corresponding valves, liquid will start flowing pushing the microbeads, but as beads are unable to pass the valve, they will accumulate next to the microvalve. Conjugated-HRP is injected in sample reservoir, making it to link to the coated beads. When reaction subtract, including TMB, is injected it will only react at functionalized bead channel. Comparing blank and reacted sample voltage output, capture antigen concentration can be computed. Reservoir *6*, Fig. 4 (a), must contain cleaning substrate, which is composed by all the reagents except for the TMB. This is because TMB is sensible to light and all the TMB must be removed from the detection channel.

The chips are designed for working on a Printed Circuit Board (PCB)-based instrument that contains the white LEDs for valve actuation and a red LED for sample detection, as shown in Fig. 5. The valve actuation LEDs are controlled by an Arduino board.

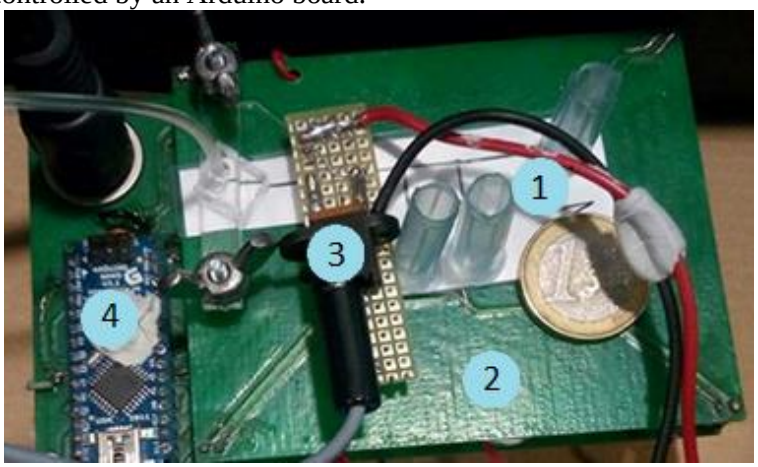

Figure 5. LoC device (1) placed onto the PCB (2) and the photodetector (3). The PCB is controlled by an Arduino Nano board (4).

Different channel/chamber geometries were considered for the detection area. A chamber area larger than the LED emitting area maximizes the sensitivity and easies the alignment of the microfluidics with the LED board. However, it also increases the chances for air trapping in the form of small bubbles (due to slower flow) or by incomplete filling of the chamber, as it was observed during experiments with these geometries. Air trapping is to be avoided due to the interference that produces in the absorbance detection, and therefore, a simple narrow channel was chosen as the more convenient geometry for the detection area.

2.5. Materials and instrumentation

Natural beeswax (melting point ~ 65 ºC) was obtained from a local candle making supply shop. Polyester transparency films for laser printers (®APLI) were purchased in a local stationary shop. ARcare® white polyester film (160μm-thick) coated on both sides with a medical grade pressure sensitive adhesive (PSA) was obtained from Adhesive Research Inc.

High Power white LEDs (LXCL-EYW4, Lumileds), red LEDs (LXZ1-PA01, Lumileds) and the photodetector (OPT101P-J) were obtained from Mouser Electronics.

For data acquisition a Data Acquisition board (DAQ) from National Instruments Corporation (NI USB-6259) was used. The cutter plotter (Camm-1 SERVO) and its cemented carbide blade (ZEC-U3017) from Roland Corp. were employed. For applying pressure, a neMESYS micropumping system from CETONI was utilized. For white LED control a Nano Arduino v3.0 was used.

3, 3′,5 ,5′-Tetramethylbenzidine liquid substrate (TMB), peroxidase from horseradish (HRP) and polystyrene micro particles (30μm) were obtained from Sigma and blue dye E131 from Acofarma. Analytical grade reagents were used to make all buffer solutions.

3. Results and discussion

The signal is obtained by differential measurements. A continuous voltage signal recording is performed, while blank and samples pass through the detection area, obtaining a continuous voltage signal. When blank passes through it, the maximum voltage value is obtained. When a sample passes through it, lower voltage value is obtained, due to the absorbance. Blank voltage (V_o) is considered to represent 0a.u. absorption sample and sample voltage (V_i) is proportional to sample analyte absorption. Thus, a step is obtained in the continuous recorded voltage, which allows to get the analytical signal. Comparing the blank voltage (V_o) and sample voltage (V_i) absorbance can be computed.

$$A = -\log_{10}(V_i/V_o) \qquad (4)$$

Although increasing LEDs power would increase the detection sensitivity, the obtained signal is limited by the maximum voltage output of the photodetector. Because of that, LED power was limited for having a maximum signal on the photodetector of 3V.

The signal statistical dispersion was computed from the voltage signal step of 3 different samples and the blank, 5 repetitions for each. The standard deviation of the obtained signal was averaged. 1.4mV was obtained. A signal must be at least 3 times greater than the dispersion for being considered the smallest distinguishable signal. Thus, the minimum distinguishable signal of the system is 4.2mV, which equals to a 0.0006a.u. absorbance.

First absorption measurements were made using a blue dye in a chip consisting in a single detection channel (without reservoirs or microvalves). Sample was injected by Flow Injection Analysis (FIA), which consists in injecting a fix volume of sample into a flowing carrier stream. For performing the FIA, 94μL were injected at 2μL/s. These measurements allowed us to know the importance of mechanical noise and the performing blank and samples measurements on the same chip.

The detection LED is placed under the microchannel and any movement of the LoC can disturb the signal. If this distortion is caused between blank and sample measurements, correct deferential measurements cannot be performed. Therefore, special care was taken to ensure the mechanical stability of the LoC on the instrument.

Every time the LoC device is placed above the detection LED different emitting areas are covered. This makes the photodetector to receive different light intensities for same samples or for the blank. However, if blank and sample measurements are performed on the same LoC device (for example, with the help of the integrated wax valves), this problem is solved. That is, there is no movement of the LoC between measurements, and therefore, the differential measurements of blank and sample are performed very accurately. This is an advantage of the present LoC approach compared with the Samsung system[23].

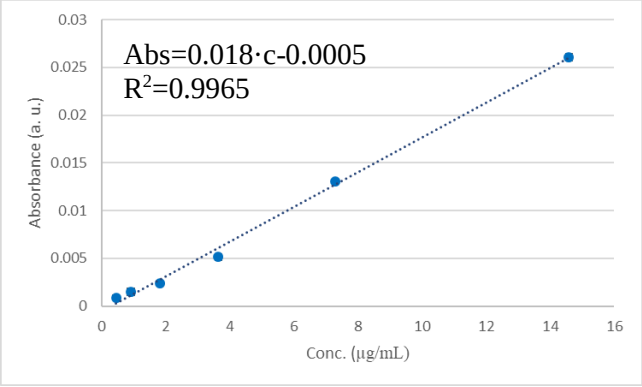

Figure 6. Calibration curve for blue dye obtained by FIA method. 94μL of different concentration sample was injected at 2μL/s for each measurement.

Fig.6 shows the calibration curve for the blue dye by FIA. The limit of detection (C_{LOD}) for the blue dye calculated as

$$C_{LOD} = 3s_{y/x} \div a \quad (2)$$

where $s_{y/x}$ corresponds to the standard error of the regression and a to the regression slope, was 1.1µg/mL.

Same set-up, unique channel chips and FIA, was used for performing initial HRP concentration measurements by the use of TMB. The TMB is a substrate that in presence of hydrogen peroxide and horseradish peroxidase (HRP) enzyme gives a blue coloured product. For measuring this product absorbance, 0.4mM and 1mM of TMB and H_2O_2 were reacted with different HRP concentrations. 4 min of enzymatic reaction was performed before injecting the solution by FIA system. 94µL were injected at 4µL/s for 100s before measuring (total reaction time of 340s). Fig. 7 (a) shows the obtained signal for three different HRP concentrations (10µg/mL, 5µg/mL and 2.5µg/mL respectively). It is very important to time the whole process for making the measurement in the same reaction point each time. The higher the HRP concentration is, the more blue product is obtained, making the obtained valley greater. Fig. 7 (b) shows a calibration curve. Absorption of TMB was measured, 0.0007a.u., without the use of HRP. This measurement must be subtracted for getting the calibration curve.

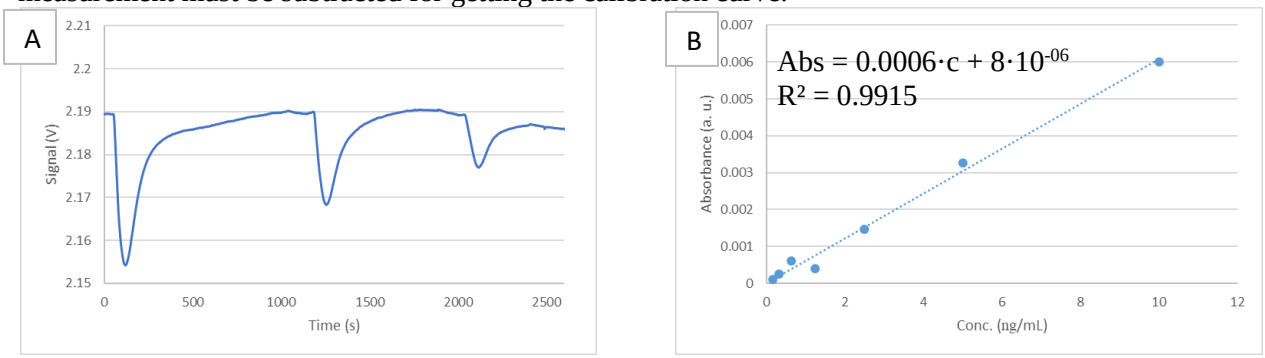

Figure 7. (a) Signal obtained for three different HRP concentrations (10µg/mL, 5µg/mL and 2.5µg/mL respectively) by FIA analysis. (b) Calibration curve of HRP. 0.4mM TMB and 1mM H_2O_2 were used.

A limit of detection of 1.1µg/mL for HRP was obtained. If we make TMB to react by using different quantities of HRP enzyme, we can compute the enzyme concentration by the Beer-Lambert Law. For that, if we consider ε as absorptivity coefficient ($3.9 \cdot 10^4$ $M^{-1} \cdot cm^{-1}$ for the blue product), l as the optical path length (160µm in our current chips), c as blue analyte concentration and A as absorbance, we know that:

$$A = \varepsilon \times l \times c \quad (3)$$

For computing the blue product concentration Michaelis-Menten kinetics can be applied. If we consider the substrate (TMB) concentration much greater than the Michaelis-Menten constant, the enzyme runs at its maximum rate ($V_{max} = [E] \cdot K_{cat}$). For a given reaction time t_r, number of enzyme molecules N_m, a catalytic constant k_{cat} ($675.6 s^{-1}$ for HRP) and volume of the reaction zone V_r, one can calculate the final concentration obtained using the equation:

$$c = N_m \cdot k_{cat} \cdot t_r / V_r \quad (4)$$

By combining equations *(3)* and *(4)* it is possible to estimate the absorbance that will be obtained for a particular number of label (enzyme) molecules. For our case, a protein purity of 27.1% and a reaction time of 340s, assuming a reaction zone of 1 µL and a 1% change in the signal received at the photodetector (equivalent to an absorbance of 0,004) corresponds to $6.2 \cdot 10^7$ enzyme molecule. That corresponds to a 4.53ng/mL, in front of the expected 6.65ng/mL. The difference can be due to different reaction conditions between the experiment and the approximation.

This way, we can relate the blue product concentration and the initial concentration of HRP, allowing an immunoassay. Once it was proved that the enzymatic reaction could be detected, dye concentration

measurements were performed on the designed microvalve equipped LoC device, Fig. 4 (a). Measurements were performed by applying a negative pressure of 30kPa at 5 for getting a flow and by performing partial opening of the valves. Each time valves were actuated a different wide small tunnel, Fig. 3 (b), was opened and, thus, different flows were achieved.

Fig. 8 shows a signal example using the LoC device. Unlike Fig. 6, flat valleys appear. This is because FIA method causes the diffusion of the sample with the flowing carrier stream. In LoC system diffusion is avoided due to the lack of a flowing carrier stream. On Fig. 8 we can see some narrow peaks which correspond to valve-actuation LED pulses.

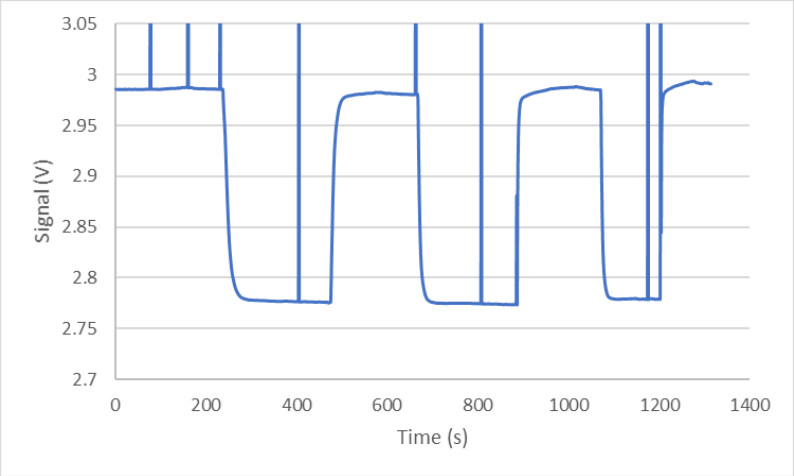

Figure 8. Signals obtained for a 17μg/mL dye sample. The upper signal value represents the blank, while de lower value represents the sample's signal. Narrow peaks are due to valve-controlling LEDs.

As previously commented, using the wax microvalves permits us to perform several measurements in a unique microchannel. This reduces alignment problems and suppose an advantage among other devices.[23] It also helps to minimize low frequency noise, ex. thermal drift, as the signal step produced by the transition between blank and sample is quite abrupt (less than 0.3 seconds as can be seen in Fig. 8).

Fig. 9 shows the calibration curve using the introduced LoC device for dye concentration measurements. We obtain a minimum detectable concentration of 1.3μg/mL for dye in LoC device. If we compare it to the ones obtained by FIA method, we see that we obtain the same resolution. In a standard microplate reader measurement, we obtain a minimum detectable concentration of 0.25μg/mL for the dye.

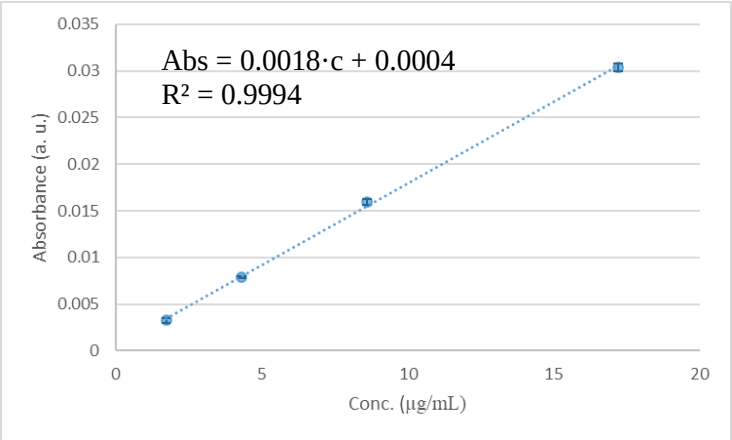

Figure 9. Calibration curve obtained for blue dye using the designed LOC device. 30kPa was applied on the chip outlet hole for getting a flow.

4. Conclusions

Although we obtain a detection five times higher than a standard microplate reader, the results are satisfactory due to the simplicity of the detection system. This simplicity makes the detection system cost-effective and easy to implement in in LOC devices. We believe that the type of assay used in the final LoC design (a bead-based enzymatic immunoassay), which is thought to produce a very large chemical signal, will compensate for the low sensitivity of the absorbance-based detection.

The use of wax microvalves allows us to make sample and blank measurements on the same microchannel, which decreases alignment and drift problems.

5. Future work

The introduced chip was designed for developing a bead-based immunoassay with the immunoreagents incorporated at the chip's reservoirs. For future development, bead-based immunoassay should be done in the designed chip. For that, a systematic study must be done for knowing the reproducibility of the bead trapping by the valve. It is crucial to get a reproducible bead trapping, as thus contain the HRP enzyme needed for the reaction, for having a reproducible reaction environment. The study should be done by varying both bead concentration and applied pressure. Once a reproducible bead trapping is reached, the immunoassay can be performed. Finally, if satisfactory results are obtained, a new LoC device with integrated reservoirs must be designed for performing on-chip the whole immunoassay.

6. Acknowledgments

I would like to show my gratitude to María Díaz and Antoni Baldi for the given opportunity and all their teaching throughout the course of this work. I would like also to thank my lab-mattes for the good working environment.

7. References

1. Manz, A.; Graber, N.; Widmer, H. M., Miniaturized total chemical analysis systems: A novel concept for chemical sensing. *Sensors and Actuators B: Chemical* **1990,** *1* (1), 244-248.
2. Sackmann, E. K.; Fulton, A. L.; Beebe, D. J., The present and future role of microfluidics in biomedical research. *Nature* **2014,** *507* (7491), 181-189.
3. Gardeniers, H.; Van den Berg, A., Micro- and nanofluidic devices for environmental and biomedical applications. *Int. J. Environ. Anal. Chem.* **2004,** *84* (11), 809-819.
4. Gardeniers, J. G. E.; van den Berg, A., Lab-on-a-chip systems for biomedical and environmental monitoring. *Anal. Bioanal. Chem.* **2004,** *378* (7), 1700-1703.
5. Kersaudy-Kerhoas, M.; Dhariwal, R.; Desmulliez, M. P. Y.; Jouvet, L., Hydrodynamic blood plasma separation in microfluidic channels. *Microfluidics and Nanofluidics* **2010,** *8* (1), 105-114.
6. Chin, C. D.; Linder, V.; Sia, S. K., Lab-on-a-chip devices for global health: Past studies and future opportunities. *Lab on a Chip* **2007,** *7* (1), 41-57.
7. Liana, D. D.; Raguse, B.; Gooding, J. J.; Chow, E., Recent Advances in Paper-Based Sensors. *Sensors* **2012,** *12* (9), 11505-11526.
8. Walsh, D. I.; Kong, D. S.; Murthy, S. K.; Carr, P. A., Enabling Microfluidics: from Clean Rooms to Makerspaces. *Trends Biotechnol.* **2017,** *35* (5), 383-392.
9. Pan, T. R.; Wang, W., From Cleanroom to Desktop: Emerging Micro-Nanofabrication Technology for Biomedical Applications. *Ann. Biomed. Eng.* **2011,** *39* (2), 600-620.
10. Azouz, A. B.; Murphy, S.; Karazi, S.; Vazquez, M.; Brabazon, D., Fast Fabrication Process of Microfluidic Devices Based on Cyclic Olefin Copolymer. *Mater. Manuf. Process.* **2014,** *29* (2), 93-99.
11. Yuen, P. K.; Goral, V. N., Low-cost rapid prototyping of flexible microfluidic devices using a desktop digital craft cutter. *Lab on a Chip* **2010,** *10* (3), 384-387.

12. Coltro, W. K. T.; de Jesus, D. P.; da Silva, J. A. F.; do Lago, C. L.; Carrilho, E., Toner and paper-based fabrication techniques for microfluidic applications. *Electrophoresis* **2010,** *31* (15), 2487-2498.
13. Focke, M.; Kosse, D.; Muller, C.; Reinecke, H.; Zengerle, R.; von Stetten, F., Lab-on-a-Foil: microfluidics on thin and flexible films. *Lab on a Chip* **2010,** *10* (11), 1365-1386.
14. Becker, H., Hype, hope and hubris: the quest for the killer application in microfluidics. *Lab on a Chip* **2009,** *9* (15), 2119-2122.
15. Díaz-González, M.; Fernández-Sánchez, C.; Baldi, A., Multiple actuation microvalves in wax microfluidics. *Lab on a Chip* **2016,** *16* (20), 3969-3976.
16. Díaz-González, M.; Boix, G.; Fernández-Sánchez, C.; Baldi, A. In *Wax microfluidics light-addressable valve with multiple actuation*, SPIE Microtechnologies, SPIE: 2017; p 102460G.
17. Pires, N. M. M.; Dong, T.; Hanke, U.; Hoivik, N., Recent Developments in Optical Detection Technologies in Lab-on-a-Chip Devices for Biosensing Applications. *Sensors* **2014,** *14* (8), 15458-15479.
18. Gustafsson, O.; Mogensen, K. B.; Ohlsson, P. D.; Liu, Y.; Jacobson, S. C.; Kutter, J. P., An electrochromatography chip with integrated waveguides for UV absorbance detection. *Journal of Micromechanics and Microengineering* **2008,** *18* (5), 7.
19. Usuba, R.; Yokokawa, M.; Ackermann, T. N.; Llobera, A.; Fukunaga, K.; Murata, S.; Ohkohchi, N.; Suzuki, H., Photonic Lab-on-a-Chip for Rapid Cytokine Detection. *ACS Sens.* **2016,** *1* (8), 979-986.
20. Llobera, A.; Wilke, R.; Buttgenbach, S., Enhancement of the response of poly (dimethylsiloxane) hollow prisms through air mirrors for absorbance-based sensing. *Talanta* **2008,** *75* (2), 473-479.
21. Rodriguez-Ruiz, I.; Conejero-Muriel, M.; Ackermann, T. N.; Gavira, J. A.; Llobera, A., A multiple path photonic lab on a chip for parallel protein concentration measurements. *Lab on a Chip* **2015,** *15* (4), 1133-1139.
22. Gielen, F.; van Vliet, L.; Koprowski, B. T.; Devenish, S. R. A.; Fischlechner, M.; Edel, J. B.; Niu, X. Z.; deMello, A. J.; Hollfelder, F., A Fully Unsupervised Compartment-on-Demand Platform for Precise Nanoliter Assays of Time-Dependent Steady-State Enzyme Kinetics and Inhibition. *Analytical Chemistry* **2013,** *85* (9), 4761-4769.
23. Lee, B. S.; Lee, J. N.; Park, J. M.; Lee, J. G.; Kim, S.; Cho, Y. K.; Ko, C., A fully automated immunoassay from whole blood on a disc. *Lab on a Chip* **2009,** *9* (11), 1548-1555.
24. Sansumg Electronics Co Ltd. 2013. LABGEO IB10. [ONLINE] Available at: http://www.samsung.com/global/business/healthcare/healthcare/in-vitro-diagnostics/BCA-IB10/DE. [Accessed 27 August 2017].
25. Rissin, D. M.; Kan, C. W.; Campbell, T. G.; Howes, S. C.; Fournier, D. R.; Song, L.; Piech, T.; Patel, P. P.; Chang, L.; Rivnak, A. J.; Ferrell, E. P.; Randall, J. D.; Provuncher, G. K.; Walt, D. R.; Duffy, D. C., Single-molecule enzyme-linked immunosorbent assay detects serum proteins at subfemtomolar concentrations. *Nat. Biotechnol.* **2010,** *28* (6), 595-599.
26. Gijs, M. A. M., Magnetic bead handling on-chip: new opportunities for analytical applications. *Microfluidics and Nanofluidics* **2004,** *1* (1), 22-40.